European Rotorcraft Forum

HELICOPTER FLIGHT DYNAMIC AXIS COUPLING IDENTIFICATION

Philipp Krämer, kraemer@dhbw-ravensburg.de, DHBW Ravensburg (Germany)

Abstract
The paper reviews the research that combines dedicated modelling approaches in a nonlinear environment with parameter estimation and system identification methods to pursue two goals simultaneously. First, the improvement of helicopter axis coupling prediction capabilities and second, to gain an insight into the physical mechanisms leading to the phenomena by analysing the identification results. Axis coupling behaviour of helicopters is discussed and the knowledge of the phenomena is compiled to lay the foundation for the modelling and simulation task. The specific modelling approach applied is based on the Parametric Wake Distortion (PWD) theory that yielded a closed mathematical formulation for the treatment of pitch-roll cross coupling. In order to make use of this combined nonlinear analytical/parametric formulation, system identification and parameter estimation methods are used to quantify the effects involved. The methods based on the maximum likelihood output error estimation are presented and explained. The actual optimisation task is applied to BO 105 flight test data and is thoroughly analysed with regard to the stated objectives. The method proved to be suited to support the goals postulated for this research. As per the two stated goals, the results are interpreted twofold. The improvement of simulation fidelity and the conclusions to be obtained regarding the involvement of the addressed physical effects. The resulting values of the estimated parameters of the optimized result yields an insight into the participation of the addressed phenomenon in the improvement of the simulation result. The paper concludes with an assessment of the methods.

1. INTRODUCTION

Flight dynamic axis coupling is a phenomenon that all helicopters experience in a more or less pronounced way. Due to its aeromechanic nature and the complex interaction of blade motion, rotor dynamics, aerodynamics, and rotor downwash propagation it is very difficult to predict the phenomenon of pitch-roll cross coupling accurately using analytical modelling means.

The simulation model is being researched at and used for academic purposes at DHBW Ravensburg University. Consequently, superior model fidelity is not to be obtained at all cost. Rather, an understanding of the phenomenology behind the observed effects is of at least the same importance. DHBW Ravensburg uses the helicopter models for piloted simulation and off-line as baseline for handling qualities, control design and systems integration work in both research and teaching. One of the facilities operated at DHBW is a full scale piloted simulation facility based on hardware and a flight model of the BO 105 helicopter including an 8 channel 90x240 deg field of view visual system, original fuselage with connected instruments, inceptors and control loading system. A moving base is currently under development.

This context drives the approaches and methods applied to specific physical problems. The paper reiterates the past research and state of the art of the subject and compiles the theoretical basis for the intended work as the foundation to achieve the objectives in current and upcoming research activities.

Copyright Statement
The authors confirm that they, and/or their company or organization, hold copyright on all of the original material included in this paper. The authors also confirm that they have obtained permission, from the copyright holder of any third party material included in this paper, to publish it as part of their paper. The authors confirm that they give permission, or have obtained permission from the copyright holder of this paper, for the publication and distribution of this paper and recorded presentations as part of the ERF proceedings or as individual offprints from the proceedings and for inclusion in a freely accessible web-based repository.

2. OBJECTIVES

The approach followed by the described research aims to combine a physics-based nonlinear modelling with parametric extensions that are implemented in a way that the parameters, and their respective values, have a physical significance regarding the addressed effects. The application of this approach to the axis cross-coupling behaviour of helicopters serves two essential aspects. On the one hand, it supports the demonstration that the nonlinear-parametric method described here is viable and can be applied efficiently. On the other hand, it attempts to contribute to current problems in helicopter flight dynamics research. Thus, this is more than a mere verification of the mathematical approach - although the problem definition was chosen with this in mind.

The Parametric Wake Distortion (PWD) model, derived and described in detail in section 5, meets these requirements. Based on physical principles, it describes the rotor downwash and its interaction with the generated loads on the rotor itself. Several parameters, also based on physical observations, whose sensitivity and magnitude are approximately known from previous work, come into play.

With this and as will be seen in the following, this model fulfils the requirements regarding the suitability for verifying the approach:

- The model is physically based and allows a conclusion to be drawn about the involvement of the corresponding effects in the various flight conditions through the values of the determined parameters.

This work is licensed under the Creative Commons Attribution International License (CC BY). Copyright © 2021 by author(s).

- A priori knowledge is available in terms of parameter sensitivity and magnitude, which produces comparable results and allows the effectiveness of the optimisation algorithm to be demonstrated.
- The model offers multiple parameters, which have to be optimised synchronously. This is a basic optimisation requirement for the nonlinear-parametric modelling approach.
- The problem originates from an area that is the focus of current research efforts of various institutions involved in helicopter research. On the one hand, this makes it possible to contribute to the current discussion and, on the other hand, enables an exchange with scientists also working in this field.

A number of publications continued the original development of wake distortion approaches and work in the field of dynamic inflow modelling[1].

The aim of this task is to optimise the Parametric Wake Distortion model based on flight test data in such a way that an improvement of the pitch-roll coupling behaviour (in both directions) becomes apparent. In order to gain a broad experience base, different flight conditions are to be used for the application. In addition to a statement about the improvement of the results, a statement about the physical effects involved is to be achieved based on the parameter values obtained. In general, this task intends to consider whether and under which conditions the combined modelling procedure is practicable and which advantages distinguish this special procedure.

3. METHODS

3.1. Simulation model

The global simulation model consists of a fully nonlinear formulation for conventional (main rotor/tail rotor) helicopter configurations. Special emphasis is placed on the modelling of the rotor hub in order to cover the inherent structural differences between individual rotor hub types. Main rotor aerodynamics is represented by a blade element momentum theory model including a baseline inflow model based on the Pitt and Peters dynamic inflow[2][3]. Approximation of the structural blade dynamics is implemented by both a rigid blade formulation as well as an elastic blade formulation covering flapping, lead-lag, and feathering (the latter being a current field of improvement).

The tail rotor model is a derived and simplified model of the main rotor covering the specifics of the tail rotor hub and the resulting effects on rotor/blade motion.

Look-up tables, yielding the aerodynamic loads based on local angles of attack and sideslip, represent the fuselage (including main rotor hub, tail boom, and skids/gear) as well as empennage aerodynamics.

The routines solving the equations of motion offer flexibility in the choice of integration routines, computation time-step adaptation, trim algorithm and precision.

3.2. Parameter estimation

The basic idea of system identification is to compare a simulated signal with measured quantities and to minimise the deviation (i.e. the error) of the signals by adjusting the parametrised simulation model – both in terms of its structure, and of estimating its parameter values.

Depending on the application and the objective, different numeric approaches are suitable for defining the error and algorithms for controlling the parameter variation. System identification and parameter optimisation can be carried out both in the time domain[4][5] and in the frequency domain[6][7][8] – again, the choice depends on the application and the available data and numerical tools. In both cases a compatibility analysis of the data should be carried out[9]. This serves to examine whether the measured data are consistent in themselves and to be able to reproduce quantities that cannot be measured but nevertheless are necessary for identification.

The comparison of the methods in[7] shows that a good agreement can be achieved in the results from time domain and frequency domain system identification. A difference in the results was seen in some specific parameters, which is due to differences in the dynamic bandwidth of the data used. On the other hand, differences in the dead times occurred due to the different optimisation approaches, which also has an impact on the estimated global Eigenmodes of the model.

3.2.1. Plant considerations

It becomes apparent that in this process much depends on the actually investigated system. Here, the helicopter presents itself as particularly demanding due to its characteristic properties.

The strong couplings of the system states require that many degrees of freedom need to be taken into account in the simulation. A division into longitudinal and lateral motion is – in contrast to the investigation of fixed-wing aircraft – difficult or even impossible to apply. Extracting transfer functions from an input to a specific output is made more difficult by the fact that the disturbing influences of the axis couplings must be taken into account or eliminated.

The high vibration level in helicopters leads to very noisy measured values, especially in acceleration and rotation rate signals. Here, an attempt must be made to filter out these vibrations from the measurement signals without influencing frequency ranges that contain useful signals and are to be included in the analysis.

Furthermore, the natural instability of the helicopter allows only short test durations. Too large amplitudes of the dynamic movements no longer fulfil the requirement to linearize, which may be necessary in many areas – especially in the context of system identification.

Another integral part of system identification is the verification of the results. For this purpose, simulation calculations are carried out with inputs from flight tests and the calculated outputs are compared with the outputs measured in the test. For the verification of identified simulation models, it is genrally not very informative to compare the simulation data with the flight tests from which

This work is licensed under the Creative Commons Attribution International License (CC BY). Copyright © 2021 by author(s).

the model was identified (except, for example, to prove the sensitivity of the identified models and parameters as being done in the present research).

Dissimilar test data, i.e. data that was not used for the optimisation itself, is therefore suitable for the verification of identified models. Good agreement can be achieved with these if the identified models and parameters describe the system well and no disturbing influences (turbulence, errors in the measurement chain, etc.) are represented in the data. This in turn presupposes that the experimental data are also comparable and have been treated in the same way for data preparation.

For the verification of identified models, it is important to take this into account, as the information content of the flight test data is reflected in the models identified with them. Thus, models identified from flight test data with "3-2-1-1 control inputs" contain more information than those identified from test data with doublets as inputs. A "higher information model" should be able to simulate "lower information trials" sufficiently well. The reverse may result in a less good match, depending on the frequency range in which the system excitation of the respective identification and verification trials took place.

3.2.2. Robustness

The concept of robustness[5] occupies a significant position in the entire application cycle of parameter optimisation and system identification. The more complex the task and the more demanding the system under consideration, the more obvious this becomes.

A list of five points[5] which are decisive for the identification of the system in the sense of robustness clarify this rather general concept:

1. robustness and reliability of the a priori information for identification and the relevance of the data used,
2. robustness of the identification procedure for defining the model structure, as well as for estimating the parameters,
3. robustness, consistency and accuracy of the identified model structure,
4. robustness, consistency and accuracy of the estimated parameters,
5. overall robustness of the resulting mathematical model.

These points clarify that system identification is a procedure that offers great potential, but in return requires great care in preparation, implementation and verification.

3.2.3. The numerical method

The choice of the estimation method and the optimisation algorithm has a significant influence on the way the routines are integrated into the simulation environment. Various methods of system identification were examined with regard to their efficiency with respect to the task at hand. The maximum likelihood method was selected from the available methods. This is a widely established method in aeronautical research, which has already led to good results in other projects.

The maximum likelihood method defines the error $\underline{e}$ at each time step k by the difference between the measurand $\underline{z}$ and the simulated (observed) output $\underline{y}$. The measurand $\underline{z}$ contains both, the measured value and the observed value. The measured variable $\underline{z}$ is composed of the measured output $\underline{y}_m$ and the measurement noise of the output variables $\underline{v}$.

$$\begin{aligned}\underline{e}(k) &= \underline{z}(k) - \underline{y}(k) \\ &= \underline{y}_m(k) + \underline{v}(k) - \underline{y}(k)\end{aligned} \tag{1}$$

Based on the error definition (1), the cost function J to be minimised is given by equation (2). The establishment of this cost function is based on the essential hypothesis that the covariance matrix of the measurement error $\underline{R}$ is known and given. This results in the adjustment of the cost function. A weighting with respect to the given a priori values $\underline{\Theta}_0$ is introduced here.

$$\begin{aligned}J\{\underline{\Theta}\} = &\frac{1}{2}\sum_{k=1}^{K}\left[\underline{z}(k) - \underline{y}(k)\right]^T \underline{R}^{-1}\left[\underline{z}(k) - \underline{y}(k)\right] \\ &+ \frac{1}{2}W\left[\underline{\Theta} - \underline{\Theta}_0\right]^T \underline{R}_0^{-1}\left[\underline{\Theta} - \underline{\Theta}_0\right]\end{aligned} \tag{2}$$

The right-hand side of the cost function contains the term $\left(W\left[\underline{\Theta} - \underline{\Theta}_0\right]^T \underline{R}_0^{-1}\left[\underline{\Theta} - \underline{\Theta}_0\right]\right)$. This can be used to consider known a priori parameter values $\underline{\Theta}_0$. Here, the factor W additionally offers the possibility to weigh this share. $\underline{R}_0$ denotes the covariance matrix of the parameter vectors, which is also to be specified. Since an exact specification of $\underline{R}_0$ is difficult, an estimate in the form of the magnitudes of the expected values of the matrix elements of $\underline{R}_0$ is often applied. A common method is to generate $\underline{R}_0$ as a diagonal matrix of the squares of the expected parameter values. If it is not possible to pre-specify $\underline{R}_0$ all together, then this entire branch can be omitted by defining $W = 0$.

While the maximum likelihood method defines the error and the cost function to be minimised, parameter optimisation requires an iteration algorithm that varies the variable parameters $\underline{\Theta}$ in such a way that the parameter values for the minimum error are reached in as few iteration steps as possible.

It became apparent early on that a first-order algorithm does not satisfy the need for the smallest possible number of iterations, especially with multiple parameters to be optimised simultaneously[10]. From the second-order methods, the non-linear Gauss-Newton optimisation algorithm was chosen.

If the estimated parameter vector $\hat{\underline{\Theta}}(I)$ is reached at the end of iteration step I, the first and second order gradients must be formed to calculate the parameters for iteration step $(I+1)$.

$$\nabla J = \frac{dJ(I)}{d\underline{\Theta}(I)}, \qquad \nabla_2 J = \frac{d^2 J(I)}{d\underline{\Theta}(I)^2} \tag{3}$$

Since the cost function J enters the calculation of the gradients as a scalar and the parameters $\underline{\Theta}$ in form of a vector, the first-order gradient results in a vector of the dimension $[\nabla J] = (1 \times N)$ and the second-order gradient

This work is licensed under the Creative Commons Attribution International License (CC BY). Copyright © 2021 by author(s).

results in a square matrix of the dimension $\left[\nabla_2 J\right]=(N\times N)$, N being the total number of parameters to be estimated. The estimated parameter vector $\underline{\hat{\Theta}}$ at iteration step $(I+1)$ is then given by equation (4).

$$\underline{\hat{\Theta}}(I+1)=\underline{\hat{\Theta}}(I)-\left(\nabla_2 J\right)^{-1}\nabla J \tag{4}$$

Applied to the cost function of the maximum likelihood method (2), the differentiation for the first-order gradient yields the relationship shown in (5) for each element $\Theta(i), i\in[1,N]$ of the parameter vector $\underline{\Theta}$.

$$\begin{aligned}\nabla J(i)=&\sum_{k=1}^{K}\left[\frac{\partial \underline{y}(k)}{\partial\Theta(i)}\right]^T \underline{R}^{-1}\left[\underline{z}(k)-\underline{y}(k)\right]\\ &+W\left[\frac{\partial\underline{\Theta}}{\partial\Theta(i)}\right]^T \underline{R}_0^{-1}\left(\underline{\Theta}-\underline{\Theta}_0\right)\end{aligned} \tag{5}$$

The first-order gradient differentiated by the elements $i,j\in[1,N]$ of the parameters $\underline{\Theta}$ results in the second-order gradient. Assuming small deviations of calculated and measured responses $\left(\underline{z}(k)\approx\underline{y}(k)\right)$ the second-order gradient yields equation (6).

$$\begin{aligned}\nabla_2 J(i,j)=&\sum_{k=1}^{K}\left[\frac{\partial \underline{y}(k)}{\partial\Theta(i)}\right]^T \underline{R}^{-1}\left[\frac{\partial \underline{y}(k)}{\partial\Theta(j)}\right]\\ &+W\left[\frac{\partial\underline{\Theta}}{\partial\Theta(i)}\right]^T \underline{R}_0^{-1}\left[\frac{\partial\underline{\Theta}}{\partial\Theta(j)}\right]\end{aligned} \tag{6}$$

From the consideration of the first-order gradients (5) and second-order gradients (6) it can be seen that the sensitivity function $\left[\partial\underline{y}(k)/\partial\Theta(i)\right]$ is directly involved. For the numerical implementation of the sensitivity function, the partial differentiation is converted into discrete differences (7). These are determined with two separate calculations for a nominal case $\underline{y}(k)=f(\underline{\Theta})$ and an incremented case $\underline{y}'(k)=f(\underline{\Theta}+\Delta\underline{\Theta})$.

$$\left[\frac{\partial \underline{y}(k)}{\partial\Theta}\right]\rightarrow\frac{\underline{y}'(k)-\underline{y}(k)}{\Delta\underline{\Theta}} \tag{7}$$

In the numerical implementation, this means that for each time step *k*, two complete simulation calculations – for the nominal and for the incremented state – are required, which underlines the need to minimise the iteration steps to be performed.

For the problem of axis cross coupling of a helicopter described in this paper, it is necessary to process several sequentially concatenated data (flight test TOPs) and to estimate the model parameters to be optimised for all test data TOPs simultaneously. In doing so, this “multi-run function” performs a trim calculation internally before each selected TOP and determines the cost function collectively for all TOPs. Using separate TOPs for separate axis inputs, the user gains the ability to simultaneously optimise those parameters that limit their sensitivity predominantly to control excitations about a specific axis.

4. HELICOPTER AXIS COUPLING

Several physical mechanisms interact in a complex way in the development of axis coupling effects of helicopters. Effects dominated by the design of the rotor hub play a large part in the coupling behaviour. This “acceleration-axis coupling”[11] is caused by the phase angle of less than 90 deg, which is caused by the flapping hinge offset of the rotor. It causes that every initiated control moment is accompanied by a coupling moment acting orthogonally. The fact that the first flapping natural frequency of a rotor blade decreases with increasing flapping hinge offset has a decisive impact here.

As a helicopter with hingeless main rotor hub, the BO 105 does not physically have flapping hinges. However, an equivalent flapping hinge offset can be applied, which corresponds to the physical properties of the rotor and allows a calculation with the same equations. It should be noted that the equivalent flapping hinge offsets of hingeless rotors are usually considerably larger than the structurally realised ones of articulated rotor hubs. Therefore, comparatively strong axis coupling effects occur in helicopters with hingeless rotors. Design measures, such as mounting the swashplate with a lead corresponding to the phase angle, can reduce the coupling effects, but cannot completely eliminate them due to different axis coupling effects[9] and their variation with flight condition.

In addition to these rotor-specific coupling mechanisms, for the sake of completeness, inertial coupling must also be counted among the design-related origins of axis coupling. However, the resulting effects are comparatively small.

In the case of a constant rate of rotation (roll and/or pitch) applied to the rotor, moments also arise orthogonal to the direction of rotation. This “rotational rate axis coupling” is independent of structural parameters such as the flapping hinge offset.

In this context, manoeuvre effects are phenomena that show their impact during transient manoeuvres. On the one hand, the variation of the rotor coning angle leads to coupling effects[11], on the other hand, an existing side slip angle can lead to the longitudinal flapping motion of the blades being aligned with the new trajectory, thus also generating a coupling moment.

The individual effects have different consequences[9], so that it is difficult to estimate the magnitude of the axis coupling, or even to clearly predict the direction in which it takes place. As discussed, many dependencies, such as the physical parameters of the helicopter and the flight condition, have a decisive influence.

In addition to the mechanisms listed here, there are aerodynamic effects that have not been mentioned so far. Since the rotor operates in a global wind field, which it simultaneously influences by its downwash, this in turn causes reactions of the rotor and thus of the generated rotor loads. The modelling of the rotor inflow is of particular importance in this context. In the following, the theory of inflow modelling briefly is discussed and the model derived with which the prediction of the axis coupling is to be improved using parameter optimisation.

This work is licensed under the Creative Commons Attribution International License (CC BY). Copyright © 2021 by author(s).

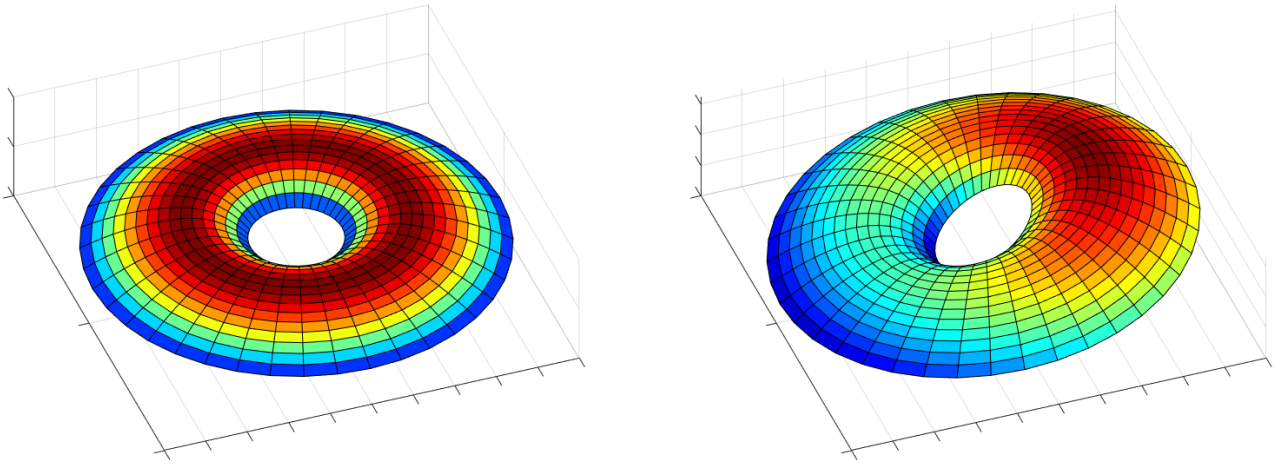

Figure 1 Qualitative distribution of induced velocities over the rotor disk area in hover flight (left) and with superimposed forward velocity (right).

5. INFLOW MODELLING

A distinction must be made between two parts of helicopter rotor downwash modelling. Indispensable for a description of the forces and moments on the rotor is the modelling of the induced velocities across the rotor azimuth and radius coordinates. This provides a two-dimensional profile of those velocities, which result from the thrust generation of the rotor in the rotor plane. These velocities in turn are part of the input variables for the load calculation on the rotor and are used accordingly in the next simulation time step.

The rotor wake propagation can be regarded as a dependent part of the model. Here it is considered how the downwash behaves after passing through the rotor and, for example, affects the airframe, external loads, the tail boom, the stabiliser and the fin, as well as the tail rotor. Likewise, the rotor downwash is important when considering ground effects. This description of the downwash propagation is based on the one hand on the induced speeds calculated over the rotor area and on the other hand on an assumption of how the downwash behaves after passing through the rotor. Essentially, the helicopter/rotor motion, the wake contraction, possibly an approach for the swirl in the downwind, as well as the external atmospheric influences are included in the considerations.

The following assessment refers to the inflow modelling in the rotor disk area. In the implementation, improved inflow models are combined with the wake propagation models in order to provide a global model improvement.

5.1. Dynamic inflow modelling

Dynamic inflow modelling extends the part of the momentum theory of the trust equation by a time dependence, which takes into account the inertia of the moving air masses for the calculation of the loads and induced velocities. This model, which dates back to the work of Pitt and Peters[2][3] and is commonly named after its developers, is still based on the relationship derived from Bernoulli's law of energy conservation and is usually described using dimensionless quantities.

The theory of dynamic inflow allows to consider transient effects at the level of the rotor disk loads. First, the averaged thrust equation from the momentum theory is written in integral notation as a function of the radius coordinate r and the azimuth coordinate ψ.

$$T = 2\rho \int_0^R \int_0^{2\pi} (v_z + v_i) v_i \, r \, d\psi \, dr \tag{8}$$

This formulation concentrating on the axial thrust T of the rotor introduces the induced velocity v_i to the airflow and also acknowledges a possible axial velocity of the rotor v_z relative to the surrounding air.

The aim now is to find a formulation that includes the three principal degrees of freedom of the loads on the rotor hub, consisting of thrust, moment about the x-axis and moment about the y-axis of the non-rotating rotor hub system. The moment components can be written analogously to (8) as follows.

$$\begin{aligned} M_x &= -2\rho \int_0^R \int_0^{2\pi} (v_z + v_i) v_i \, r^2 \sin(\psi) \, d\psi \, dr \\ M_y &= -2\rho \int_0^R \int_0^{2\pi} (v_z + v_i) v_i \, r^2 \cos(\psi) \, d\psi \, dr \end{aligned} \tag{9}$$

Here the signs are chosen in such a way that $M_x > 0$ causes as primary response a roll to the right and $M_y > 0$ causes a pitch-up. In this context, the distribution of the induced velocities $v_i = v_i(r, \psi)$ over the rotor disk area is important.

A common trapezoidal inflow distribution[12] is given by equation (10), where a distinction is made between the uniform (v_0), the longitudinal (v_c) and the lateral component (v_s). A corresponding inflow distribution underlies the visualisation in Figure 1.

$$v_i(r, \psi) = v_0 + v_c \frac{r}{R} \cos(\psi) + v_s \frac{r}{R} \sin(\psi) \tag{10}$$

In the case of a superimposed in-plane flow, e.g. when the helicopter is executing forward flight, the downwash field is distorted according to Figure 1, right. Here the rotor is exposed to a lateral flow from the front left and which causes an inclination of the trapezoidal inflow field (and of

This work is licensed under the Creative Commons Attribution International License (CC BY). Copyright © 2021 by author(s).

the thrust vector) into the direction of the lateral flow. Thus, the longitudinal and lateral components, v_c and v_s, are no longer zero, as assumed in the left part of Figure 1.

This approach constitutes a purely trapezoidal inflow distribution across the rotor disk area, given the strict cosine and sine relations with the azimuth coordinate ψ. Other "classical" approaches go beyond a pure trapezoidal assumption, such as those of Beddoes (a vortex lattice method that includes single blade effects) or Mangler-Squire (a higher-harmonic method that does not consider discrete single effects).

The momentum theory equations can now be transformed into a dimensionless notation by introducing load coefficients C and inflow ratios λ instead of the unitary variables according to the following definition.

$$C_T = \frac{T}{\rho S \Omega^2 R^2}, \quad C_l = \frac{L}{\rho S \Omega^2 R^3}, \quad C_m = \frac{M}{\rho S \Omega^2 R^3}$$
$$\lambda_0 = \frac{v_0}{\Omega R}, \qquad \lambda_s = \frac{v_s}{\Omega R} sin(\psi), \quad \lambda_c = \frac{v_c}{\Omega R} cos(\psi) \tag{11}$$

Following this notation, the vertical speed of the rotor, or its relative vertical flow, v_z, which is added to the induced speed v_i, is employed in dimensionless form as $\lambda_z = -v_z / (\Omega R)$. The negative sign here takes into account the relative incident flow from the rotor coordinate system compared to the wind axis system. Furthermore, it should be mentioned that the investigation is limited to the first harmonic form ("1 per rev"). Higher harmonic functions can be neglected here with the aim of a flight mechanical application of the models[2].

In equation (11) C_T describes the thrust coefficient in z-direction and C_l and C_m the moment coefficients at the rotor hub about the local, helicopter-fixed x- and y-axes, respectively. λ_0 denotes the portion of the local induced velocity independent of the azimuth coordinate, while λ_s describes the distribution of the induced velocities in the direction of the y-axis and λ_c that in the direction of the x-axis. With these six variables, all main loads acting on the rotor hub, as well as the entire induced velocity field in the rotor disk plane, are covered. Taking into account the vertical speed of the helicopter at the rotor hub λ_z, conditions for these three degrees of freedom must now be established from both the momentum theory and the blade element theory, just as in the one-dimensional case.

Applied to the equation of the momentum theory, a notation in dimensionless quantities can be set up for all three degrees of freedom (12).

$$\begin{bmatrix} C_T \\ C_l \\ C_m \end{bmatrix} = \hat{\underline{L}}^{-1} \begin{bmatrix} \lambda_0 \\ \lambda_s \\ \lambda_c \end{bmatrix} \tag{12}$$

It should be noted that the load coefficients given here represent purely aerodynamic loads. Inertial loads are not considered at this point. The gain matrix $\hat{\underline{L}}$ now contains the terms that relate the load coefficients to the induced velocities or the flow rates. A detailed derivation of the elements of $\hat{\underline{L}}$ exists for arbitrary incidence flow conditions at the rotor [3]. In the simplest case, i.e. for a pure vertical movement of the rotor without lateral components of the surrounding airflow, the gain matrix $\hat{\underline{L}}$ assumes a diagonal form and contains only the transfer functions $\lambda_0 \rightarrow C_T$, $\lambda_s \rightarrow C_l$ and $\lambda_c \rightarrow C_m$.

Taking into account an additional lateral flow to the rotor, $\hat{\underline{L}}$, on the other hand, is fully occupied and thus completely describes the couplings through the induced velocities between the three degrees of freedom for the loads on the rotor. This formulation thus makes a direct contribution to the description of the axis coupling behaviour due to aerodynamic inflow effects on the main rotor.

According to the first line in equation (13), $\hat{\underline{L}}$ is composed of a matrix $\underline{L}$, which contains the angles of incidence at the rotor, and an inflow parameter matrix $\underline{V}$, in which the total rotor flow rate and the mass flow rate parameters due to cyclic variations are represented. The second line in equation (13) again indicates the assignment of these two matrices for the case that only a vertical external flow v_z occurs at the rotor (v_x = v_y = 0), i.e. the rotor performs a vertical but no lateral movement relative to the surrounding air.

$$\hat{\underline{L}}^{-1} = \underline{V}\,\underline{L}^{-1}$$
$$\hat{\underline{L}}^{-1} = \begin{bmatrix} \lambda_0 - \lambda_z & 0 & 0 \\ 0 & 2\lambda_0 - \lambda_z & 0 \\ 0 & 0 & 2\lambda_0 - \lambda_z \end{bmatrix} \begin{bmatrix} \frac{1}{2} & 0 & 0 \\ 0 & 2 & 0 \\ 0 & 0 & 2 \end{bmatrix}^{-1} \tag{13}$$

Expanded, the following assignment results for the amplification matrix $\hat{\underline{L}}$.

$$\hat{\underline{L}}^{-1} = \begin{bmatrix} 2(\lambda_0 - \lambda_z) & 0 & 0 \\ 0 & \lambda_0 - \frac{1}{2}\lambda_z & 0 \\ 0 & 0 & \lambda_0 - \frac{1}{2}\lambda_z \end{bmatrix} \tag{14}$$

If this diagonal matrix is applied to equation (12) , the following relationship explicitly results.

$$C_T = 2(\lambda_0 - \lambda_z)\lambda_0$$
$$C_l = (\lambda_0 - \tfrac{1}{2}\lambda_z)\lambda_s \tag{15}$$
$$C_m = (\lambda_0 - \tfrac{1}{2}\lambda_z)\lambda_c$$

If the definitions of the dimensionless quantities from equation (11) are now inserted into these relationships, the first line directly results in that of the thrust equation of the one-dimensional momentum theory, which verifies the approach presented here. As indicated, the 3-degree-of-freedom consideration of momentum theory becomes considerably more complicated when lateral inflows in the rotor disk plane are taken into account.

Compared to (12), the model of the dynamic inflow now introduces a time-dependent term in order to account for the acceleration of the air masses.

$$\begin{bmatrix} C_T \\ C_l \\ C_m \end{bmatrix} = \underline{M} \begin{bmatrix} \dot{\lambda}_0 \\ \dot{\lambda}_s \\ \dot{\lambda}_c \end{bmatrix} + \hat{\underline{L}}^{-1} \begin{bmatrix} \lambda_0 \\ \lambda_s \\ \lambda_c \end{bmatrix} \tag{16}$$

Thus, the purely algebraic relationship (12) becomes an inhomogeneous, first order linear differential equation (16), which can be solved for each time step of a simulation with

This work is licensed under the Creative Commons Attribution International License (CC BY). Copyright © 2021 by author(s).

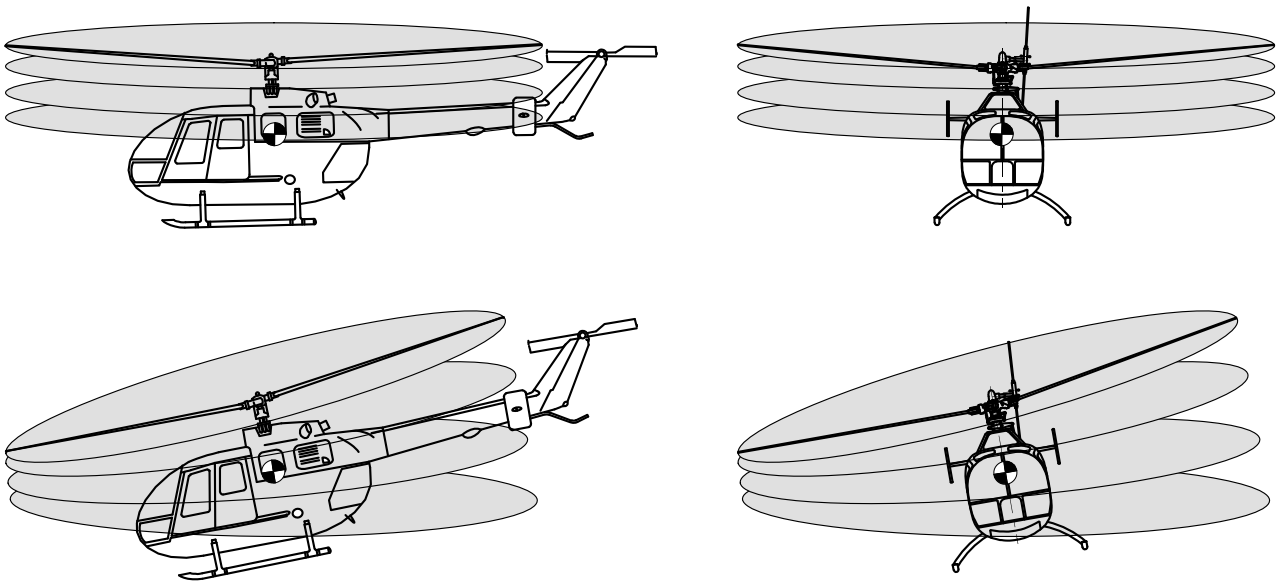

Figure 2 Principle of wake propagation with pitch and roll motion in hovering flight[9].

constant coefficients. The acceleration term is based on the Newtonian relationship between load and accelerated, inertial mass. Therefore, the elements of the matrix M introduced here assume the function of an “apparent” mass, or inertia, which, however, are introduced without dimensions.

Pitt and Peters[2] describe the derivation of this "apparent mass matrix" as the result of an approximation of the pressure distribution over the rotor disk area by Legendre polynomials, which goes back to the work of Joglekar, Loewy and Kinner[13]. Pitt and Peters prove the applicability of the given dimensionless pressure distributions $\Phi(\psi,r)=p/\left(\rho\Omega^2R^2\right)$ to the linear first order problem of dynamic inflow modelling. The Legendre formulation directly results in a constant occupancy of the apparent mass matrix $\tilde{\underline{M}}$ in the rotor plane, given in (17).

$$\tilde{\underline{M}}=\begin{bmatrix}\frac{8}{3\pi} & 0 & 0\\ 0 & -\frac{16}{45\pi} & 0\\ 0 & 0 & -\frac{16}{45\pi}\end{bmatrix} \tag{17}$$

In order to focus the results on the problem of helicopter rotors, Pitt and Peters propose a corrected pressure distribution compared to the matrix $\tilde{\underline{M}}$. This is adapted to the special case by assuming a pressure at the location of the rotor hub of $\Phi(\psi,r=0)=0$ due to the rotor operation, as well as a horizontal tangent at the same location in the direction of the radius coordinate $\partial\Phi(\psi,r=0)/\partial r=0$. This assumption, justified among other things by the twist of the rotor blades, leads to a corrected apparent mass matrix $\underline{M}$ which is shown in (18).

$$\underline{M}=\begin{bmatrix}\frac{128}{75\pi} & 0 & 0\\ 0 & -\frac{256}{945\pi} & 0\\ 0 & 0 & -\frac{256}{945\pi}\end{bmatrix} \tag{18}$$

It is worth noting that the resulting apparent mass matrices are diagonal for all the pressure distribution approaches considered and the second and third elements on the principal axis are identical.

The dynamic inflow model improved the prediction of the induced velocities and the rotor thrust considerably since its conception. Especially with regard to the effects of unsteady, transient control inputs and state changes, it thus made a valuable contribution to improving the simulation quality of helicopter models especially when addressing axis-coupling phenomena as will also become evident when assessing the Parametric Wake Distortion approach.

5.2. Parametric wake distortion

The inclusion of a dynamic acceleration term makes it possible to describe the thrust generation of manoeuvring helicopters considerably better, since the acceleration forces of the air masses, as was shown, are not negligible. However, this improvement was mainly effective in forward flight. In hovering flight and in slow horizontal flight, there was still potential for improvement after the introduction of this model[9].

A promising approach was achieved by feeding back the two rotational degrees of freedom of the main rotor (pitch and roll) into the inflow equation. An essential basis for this was created by the work of Keller and Curtiss[14][15], who scaled the feedback via a free parameter K_R. This created the basic formulation of “Parametric Wake Distortion” modelling, with the specific aim of achieving an improvement in the prediction of axis cross coupling.

Figure 2 illustrates the principle of the wake distortion theory. When a helicopter is in hover, the tip vortices generated at the blade tips propagate symmetrically downward. This condition is shown in Figure 2 in the upper half in the side view and in the front view. We will now look at manoeuvres that distort the downwash asymmetrically. Two cases come into consideration.

This work is licensed under the Creative Commons Attribution International License (CC BY). Copyright © 2021 by author(s).

1. translational manoeuvres, also relative changes of state with respect to the surrounding atmosphere, which do not act in the direction of the symmetry axis of the downwash (i.e. the rotor vertical axis) and shift the wake "outwards" in a direction below the rotor plane.

2. rotational manoeuvres, e.g. due to cyclic control inputs, which do not act around the downwash symmetry axis and compress the rotor wake on one side and expand it on the opposite side.

A translational change of state causes the centres of the vortex core lines as they depart from the blade tips to no longer lie on the extension of the rotor axis, resulting in an uneven induction of the velocity field in the rotor plane.

In terms of the coupling effects studied, rotational manoeuvres have much greater consequences, as can be seen from section 4, which is why the main focus in the following lies on these manoeuvres. Here, the vortex core lines are compressed on one side of the rotor wake and pulled apart on the opposite side. In Figure 2, the bottom line illustrates this condition for a transient pitch motion (left), as well as a roll motion (right).

The approach assumes that the uneven compression, or expansion, of the vortex field in the wake of the rotor exerts an influence on the induced velocity field surrounding the rotor. This manipulation of the inflow field thus has a direct effect on the effective angles of attack at the blade elements of the rotor, which in turn leads to changed loads at the blade elements and thus in the entire rotor system. The axis coupling mechanisms described in section 4 then cause an impact on the coupling behaviour of the helicopter.

This phenomenological description makes it clear that the approach of wake distortion suggests to be applied to helicopters which have a high degree of axis coupling due to their design. This includes helicopters with a hingeless rotor hub design, such as the BO 105.

The development of a mathematically closed formulation was based on the theoretical work of Rosen and Isser[16]. Later followed an applied model, which introduces a feedback of the rotational effects as well as the translational effects to the rotor inflow[14][17]. Hamers and von Grünhagen[18] introduced the closed formulation (19) as an extension of the dynamic inflow model (16) of Pitt and Peters.

$$\underline{M}\begin{bmatrix}\dot{\lambda}_0\\ \dot{\lambda}_s\\ \dot{\lambda}_c\end{bmatrix}+\underline{\hat{L}}^{-1}\begin{bmatrix}\lambda_0\\ \lambda_s\\ \lambda_c\end{bmatrix}=\begin{bmatrix}C_T\\ C_l\\ C_m\end{bmatrix}+\frac{K_R}{\Omega}\underline{\hat{L}}^{-1}\begin{bmatrix}0\\ p-\dot{\beta}_s\\ q-\dot{\beta}_c\end{bmatrix} \tag{19}$$

The vectorised terms added on the load side of equation (19) describe the relative motion of helicopter and blade tip plane about the roll axis $\left(p-\dot{\beta}_s\right)$, as well as about the pitch axis $\left(q-\dot{\beta}_c\right)$, with β_s, β_c representing the rotor disc inclination in roll and pitch, respectively, based on the blade flapping angles $\beta(\psi)$. The gain matrix $\underline{\hat{L}}$ explained above must also be included in this added term, according to its definition by Pitt and Peters. The parameter K_R related to the rotor speed Ω is used to scale the relative rates of the blade's tip path plane that is fed back to the load vector ($[C_T\ C_l\ C_m]^T$). The scaling factor K_R thus offers the possibility of a parametric analysis of the physically occurring interaction of rotor wake distortion and load balance at the rotor hub. Keller offers a value of $K_R = 1.5$ as a result of his theoretical observations[14].

The model approach with a single feedback parameter appears to be predominantly useful for observations in hover flight. In this condition, the only difference for the downwash description around the two axes is the different influence by the fuselage flow interaction, as well as the difference in the helicopter reaction caused by different inertia about the axes, which is, however, implicitly considered in equation (19).

However, the conditions develop differently in horizontal flight. In this case, the downwash is shifted in "backward" direction below the rotor plane. A superimposed roll or pitch rate leads to different responses about the two axes in response to the wake distortion effect. An obvious extension of the model was to split the model into separately scaled components around the roll and pitch axes. Equation (20) introduces for this consideration the wake distortion parameters K_p and K_q.

$$\underline{M}\begin{bmatrix}\dot{\lambda}_0\\ \dot{\lambda}_s\\ \dot{\lambda}_c\end{bmatrix}+\underline{\hat{L}}^{-1}\begin{bmatrix}\lambda_0\\ \lambda_s\\ \lambda_c\end{bmatrix}=\begin{bmatrix}C_T\\ C_l\\ C_m\end{bmatrix}+\frac{1}{\Omega}\underline{\hat{L}}^{-1}\begin{bmatrix}0\\ K_p\left(p-\dot{\beta}_s\right)\\ K_q\left(q-\dot{\beta}_c\right)\end{bmatrix} \tag{20}$$

The two introduced parameters weigh the coupling reactions separately. The parameter K_p is responsible for the feedback of the reaction of a roll control input to the pitch rate and K_q for the feedback of the reaction of a pitch control input to the roll rate.

In this sense, the newly introduced parameters coincide with the formulation (19) in that they assume $K_p = K_q = K_R$ according to the theory applied for hover flight. In forward flight it can be assumed that with increasing speed the rotor wake is increasingly pushed out of the sphere of influence of the rotor and the effect diminishes until, as a result, the parameters $K_p = K_q = 0$ can be assumed for higher flight speeds.

With regard to the system identification procedure, the Parametric Wake Distortion model offers several decisive aspects which qualify it for this application. First and foremost, it is a model that describes a physical situation by means of a variable parameter. As shown above, theoretically unambiguous values can be derived for the boundary conditions hovering flight and fast forward flight. The value of the parameter provides direct information about the extent to which the effect under investigation is involved in the load budget of the helicopter rotor over the entire speed range.

In addition, the model can be equipped with multiple parameters that are sensitive to the problem. The ability to estimate several parameters simultaneously can be considered as a basic competence of the optimisation routine as part of the integrated modelling procedure. The multi-run capability must be used in order to be able to consider test data adapted to the individual parameters simultaneously in a single optimisation run.

This work is licensed under the Creative Commons Attribution International License (CC BY). Copyright © 2021 by author(s).

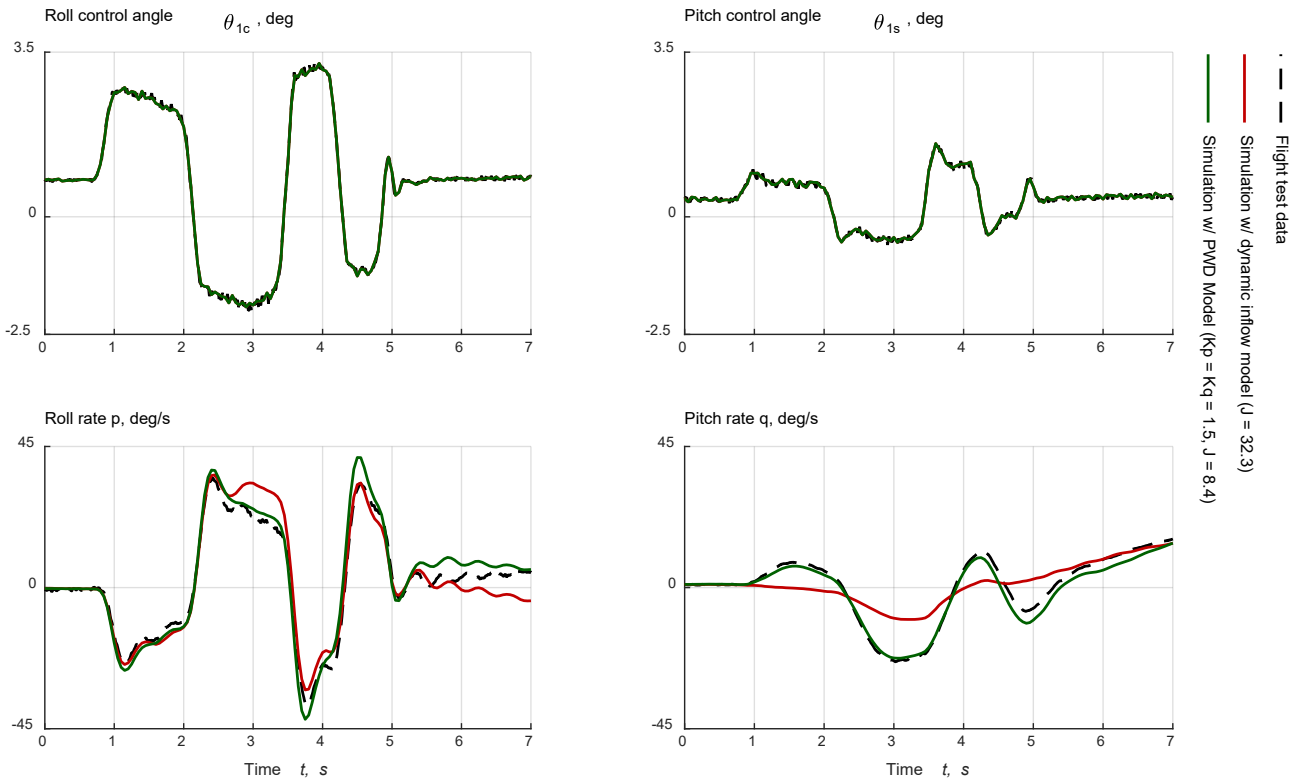

Figure 3 Effect of the PWD model on simulation fidelity – BO 105, hover, swashplate controls, 3-2-1-1 input signal.

6. RESULTS

This section presents the results obtained by implementing the Parametric Wake Distortion Model (20) and optimising the parameters K_p and K_q contained therein. This analysis is applied to the BO 105 helicopter, which has a number of distinctive features for this application:

- Due to the hingeless main rotor hub with a comparatively high equivalent flapping hinge offset, the BO 105 is exposed to strong axis couplings. As explained previously, this implies that a large effective amount of wake distortion on the axis coupling is to be expected.
- The available overall model of the BO 105, in which the Parametric Wake Distortion model is integrated, has a fairly high overall simulation quality. Therefore, it may be assumed that parasitic influences from other model deficits to flow into the estimated parameters to only a relatively small extent. This assumption hast to be challenged when interpreting the results.
- The available experimental database[19] is characterised by high quality and integrity. The measurement data from flight tests generated within the framework of the international GARTEUR working group were generated and processed specifically with data quality aspects in mind.

From the selection outlined in section 3.1 a model is composed, which is suited to the requirements of the application discussed. In addition to the naturally required selection of the dynamic inflow model as reference, which is compared here to the Parametric Wake Distortion Model, a rigid rotor blade formulation is applied for the simulation. The flapping and lead-lag motion of the blades is taken into account by an equivalent first-order spring-mass-damper system with two degrees of freedom (the flapping angle β and the lead-lag angle ζ), but the Eigenmotions of the blades themselves are neglected. This is assumed permissible because the influence of elastic blade models on the simulation quality of flight mechanical investigations plays a rather subordinate role[9]. Calculations addressing other objectives (e.g. noise and vibration calculations, as well as investigations of rotor dynamics) require a corresponding formulation of elastic blades.

6.1. Optimisation results BO 105, hover

6.1.1. Model verification results

First, the effects of the pure implementation of the Parametric Wake Distortion ("PWD") model with nominal parameters will be investigated. For this purpose, the parameters K_p and K_q are set to the theoretically derived values of $K_p = K_q = 1.5$ determined by Keller[14] and the simulation results are compared with the recorded flight test data for a hover case. In addition, a comparison is made with those simulation results which were generated with the pure dynamic inflow modelling of the dynamic downwash (16).

Figure 3 shows this result. Depicted in the upper row are the control inputs. In the case shown, these are the swashplate angles, which represent the cyclic control commands at the rotor hub. Here Θ_{1c} describes the input for the pitch control about the lateral axis and Θ_{1s} the input for the roll control about the longitudinal axis. The control

This work is licensed under the Creative Commons Attribution International License (CC BY). Copyright © 2021 by author(s).

commands measured in flight test are fed to the model as simulation inputs. Then the measured outputs are compared with the simulated outputs (in this case the roll and pitch rates, respectively). In the bottom line of the figure, the roll rate p (as primary response to a cyclic roll control) and the pitch rate q are found as system outputs of the helicopter.

With the aim of achieving an improvement in the prediction of the axis coupling behaviour through the introduction and optimisation of the PWD model, these two system outputs, roll rate and pitch rate, are used in the following to form the optimisation criterion. Against this background, the evaluation of the simulation result in these two variables is of particular importance. The optimisation criterion itself corresponds to a quadratic optimization criterion, which represents the enclosed areas between the measured and simulated system outputs. The optimisation routine tries to minimise this area criterion by a suitable choice of parameters.

The different curves overlaying each other represent the respective data of the flight test (dashed black line), the simulation with the conventional dynamic inflow model according to Pitt and Peters (solid red line), and the simulation using the PWD model with nominal parameter values (solid green line). For the sake of clarity, all the following figures are formatted in the same way (black for the flight test, red for the simulation with a reference model and green for the simulation with the modelling improved by the contributions elaborated here).

Discrepancies between measured variables and simulation outputs, as well as drifts resulting from numerical integration, can be neutralised by keeping a constant offset between the control inputs of measurements and simulations. In the figures, this offset of the controls is removed, as they do not contribute any additional information and tend to overload the representation.

The control input in Figure 3 is a pure input command about the roll axis. The fact that the pitch control angle Θ_{1s} does not remain at the trim value results from the fact that the phase shift of the flapping motion of the blades is represented in the swashplate angles. If the pilot executes a pure roll control command with the cyclic stick, this input is distributed both, to the longitudinal and lateral pitch of the swashplate according to the reference phase angle of the BO 105 of 67 deg.

Figure 3 shows that the primary response (the roll rate p, bottom left) is simulated relatively well by both the dynamic inflow model (red), and the model with Parametric Wake Distortion "PWD" formulation (green). While the PWD model agrees slightly better with the flight test (black) in the holding phase of the second pulse (second 2 to 3.5), a slight overshoot can be seen at the beginning of the holding phase of the third pulse (around second 3.5).

After completion of the control input, i.e. starting from second 5, a slight divergence of the dynamic inflow simulation, as well as a deviation of the PWD model, is noticeable. This behaviour is not unusual for helicopter simulations, especially for hover. The instability of the helicopter in hover leads to the fact that small deviations from the trimmed state bring the helicopter out of equilibrium and the pilot has to stabilise the machine by (small) control inputs. The simulation model behaves accordingly. As can be seen from the recorded flight test data, the helicopter remains relatively stable even without significant control input. A small deviation in the simulation states integrated up to that point around second 5.5 leads to slightly divergent behaviour of the simulated response in the case considered. The oscillations that are recorded in the roll rate after second 5.5 can be attributed to an air resonance excitation.

This fact must be taken into account when optimising the parameters. Optimisation of the parameters only makes sense if the system response, with which the cost function is formed, does not diverge in the way described. Since the described divergence arises from the integration of state deviations, a parameter estimation in this time range would falsify the parameter values, since the deposition between experimental data and simulation does not originate from the investigated effects, which are to be captured with the parametric model.

The coupling response (the pitch rate q, bottom right) shows a clear improvement in simulation fidelity through the introduction of the Parametric Wake Distortion model. While the dynamic inflow model at best only slightly reproduces the trends, the simulation with the PWD formulation also achieves a very good prediction of the amplitudes. From second 3.5 onwards, a slight drift is visible, which shifts the simulated system response towards negative pitch rates. This is also due to integrated smaller deviations in the system states.

In view of this result, it can already be anticipated that the Parametric Wake Distorion model is quite capable of fulfilling the set task, the improvement in the simulation of the axis coupling behaviour. Yet, this can only be shown in Figure 3 for the pitch coupling due to roll. The aim of the PWD model is, however, to estimate the two parameters K_p – responsible for the feedback of the rolling motion to the pitching behaviour – and K_q – for the feedback of the pitching motion to the rolling behaviour – simultaneously and for both coupling directions. For this reason, the already mentioned multi-run capability of the simulation must be used for the parameter estimation. The aim is to concatenate a flight test file with pitch control input and another with roll control input and to carry out the optimisation for both flight test cases simultaneously.

6.1.2. Optimisation results

Figure 4 shows a result generated in this way. The first thing to notice is that there is a certain amount of control activity over the entire simulation period. As in the previously discussed case, these again are pure control inputs, first about the pitch axis, followed by the roll axis.

The aim of using swashplate angles instead of pilot control signals is to avoid the influence of the control chain model. When using pilot stick signals, the control chain between the stick deflection and the generated blade pitch angle is included in the simulation. Any deficiencies of the control chain model therefore also affect the simulation result. When using parameter optimisation, these model deficits have a negative influence on the optimisation results, as the Parametric Wake Distortion model investigated is not suitable to compensate for the errors in the control chain

This work is licensed under the Creative Commons Attribution International License (CC BY). Copyright © 2021 by author(s).

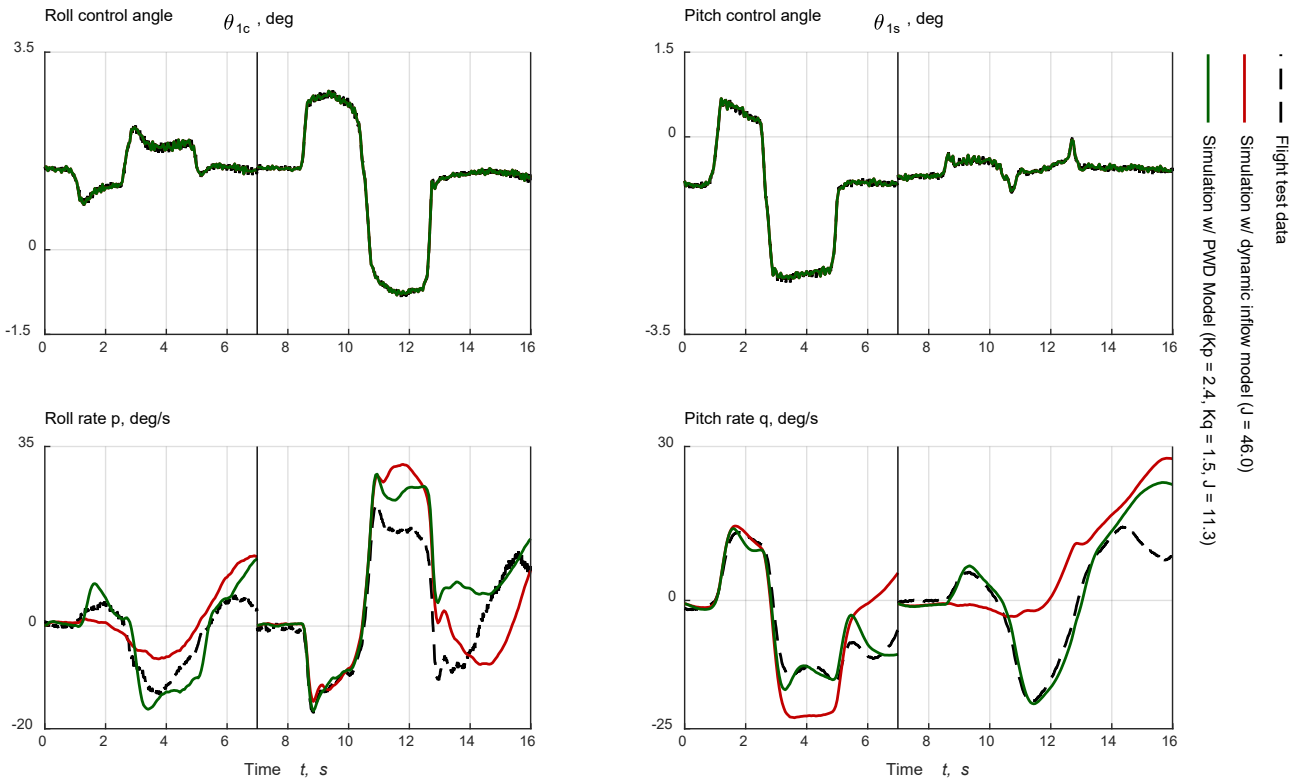

Figure 4 Simulation result with optimised PWD model – BO 105, hover, swashplate control, doublet/doublet input signal.

model. The result would be parameter values that are polluted by this circumstance.

This result of a multi-run optimisation first shows a pitch manoeuvre in the range between second 0 and 7, followed by a roll manoeuvre, starting at second 7. These are separately generated data. A trim calculation takes place before both TOPs, which means that the individual output signals do not merge at the interface between the runs.

The possible control signals differ in the frequency bandwidth of the system excitation and in the information content of the generated measurement data[9]. As has been shown, the 3-2-1-1 signal represents a good compromise between flyability and excitation bandwidth. In practical application, however, corresponding test data are not available in all flight conditions to be investigated. Furthermore, it must be assessed whether the higher value of the input signals outweighs other potential deficits in the recorded data (e.g. insufficiently trimmed output conditions or external disturbances). These considerations mean that not all optimisation calculations can use test data with optimal input signals. For reasons of the greatest possible overall quality of the investigation, experimental data were therefore selected which in this case have doublets as control input signals.

In order to be able to successively discuss the phenomena to be observed, the results are described starting with the primary responses, followed by the coupling responses, which the Parametric Wake Distortion model predominantly targets. Firstly, when looking at the simulation results in the lower half of Figure 4, it is noticeable that the pitch rate *q* (bottom right) due to the cyclic pitch control input, i.e. the primary response or "on-axis response", between seconds 0 and 7 is reproduced relatively well by both the Pitt and Peters model and the Parametric Wake Distortion model. Around second 4, however, the simulation with the dynamic inflow model overshoots significantly and only comes back into agreement with the test data after the control deflection is reduced (at second 5). The optimised simulation with the PWD model also overshoots at first, but is then forced to fit the measured output by adjusting the model parameters. This effect is not in the actual interest of the model approach to improve the prediction of the axis coupling behaviour. Obviously, the simulation result is only sensitive to a variation of the parameters in the sense of a real improvement of the simulation quality in a limited range of this section. This behaviour leads to excessive parameter values, because the optimisation algorithm tries to locally minimise the error criterion by strongly increasing the parameter values that are less sensitive to this effect, which can only succeed to a limited extent. After completion of the control input (from about second 5), however, it can be seen that the test result is predicted much better by the optimised PWD model. So that, at least in some areas, an improvement can also be recorded in the primary response.

The primary response due to the roll control input, the roll rate *p* (bottom row, left diagram) between seconds 7 and 16, shows similar effects as the pitch control primary response. Between seconds 10.5 and 12.5, an overshooting of both model responses is again recognisable, whereby an attempt is made to force a minimal deviation by means of parameter optimisation. The first control deflection around second 9 could be simulated quite well, as with the roll control primary response. After

This work is licensed under the Creative Commons Attribution International License (CC BY). Copyright © 2021 by author(s).

completion of the control input, from second 13, the roll response shows strong differences between the two simulations, as well as compared to the flight test data. Both model responses experience a renewed increase in the roll rate immediately after the completion of the control input, whereby the PWD model predicts this earlier than the dynamic inflow model. In the following three seconds of the remaining simulation time, both models are more or less inadequate compared to the simulation quality that could be achieved in the control input period.

Two phenomena can be held responsible for this. Firstly, the already discussed consequences of a departure from the trim state after a control manoeuvre in hover, which can lead to divergent results. On the other hand, inaccuracies and deficits in other areas of the overall model, which repeatedly come to bear in the course of the investigations. This is also supported by the fact that both model approaches deliver equally inaccurate results.

The coupling responses show clearly different qualities in their results. The coupling response to the pitch control input between second 0 and 7, the roll rate p in the left diagram of the bottom row, directly shows that the modelling and simulation of the off-axis response requires special care. The results obtained with the dynamic inflow model show only a low correlation with the test results, which is increased by the application and optimisation of the PWD model, but still appears to be improvable.

The coupling response to the roll control input can be seen in the pitch rate q, in the lower right of the figure between second 7 and 16. This time plot shows very clearly the potential that lies in the use of the Parametric Wake Distortion approach and its optimisation. The simulation response of the dynamic inflow model shows only a very limited correlation with the recorded test data. The PWD model, on the other hand, shows an almost perfect agreement between simulation and test data, which is only impaired by the overshooting of the amplitudes after the two control inputs, as well as the divergence of the results after completion of the control input, for the reasons already discussed. This shows both the effectiveness of the model and the sensitivity of the parameters.

First, however, we will briefly discuss the quantifiable improvement in simulation quality provided by the PWD model compared to the dynamic inflow model. The value of the cost function (the criterion J) makes it possible to form a statement about the simulation quality of the models used. The prerequisite for this is that the conditions are identical when calculating the cost function, i.e. the same parameters are used, the time range of the optimisation is identical and the weighting of the cost function with regard to the parameters is the same. This makes it clear that this is a purely relative possibility of quantification and no absolute statement can be made about the simulation quality of a particular model.

An examination of the optimised parameters for Figure 4 shows that they are close to the theoretical values: $K_p = 2.4$, $K_q = 1.5$. The relative reduction of the cost function shows a decrease of $\Delta J = 75\%$. This improvement can be explained by the fact that the simulation quality with the PWD model is relatively high, especially in the pitch response.

In the two cases discussed so far, there is the problem of divergent results after the control inputs are completed. In the following section, the Parametric Wake Distortion model is applied to forward flight. Since the static instability of a conventional helicopter tends to decrease with increasing airspeed (while dynamic instabilities increase at higher speeds), this behaviour can be expected to be reduced in level flight.

6.2. Optimisation results BO 105, forward flight

As explained in section 5.2, according to the theoretical definition of the Parametric Wake Distortion approach, it is assumed that the effectiveness of the described phenomenon decreases with increasing horizontal speed and finally disappears as the blade tip vortices are dragged backwards, out of the sphere of influence of the helicopter and its rotor. It therefore makes sense to compare this theoretical statement with the results of the parameter optimisation.

In the following, shown in Figure 5, the optimisation of the PWD model is applied to a flight condition at 80 kts forward flight speed. Again, this is a multi-run optimisation with a pitch control doublet followed by a roll control pulse as simulation input.

The primary responses, as in hover, show no substantial improvement in simulation quality by optimising the PWD model over the dynamic inflow formulation. There are slight deviations in the correct prediction of the amplitudes and the gradients in this range, mainly in the peaks of the control signals, both around the pitch and the roll axis. In detail, these are the pitch rate around second 2 and between second 3 and 4, as well as the roll rate from second 7 and around second 8. In the latter case, the amplitude is clearly better matched by the PWD model than by the dynamic inflow model, but an oscillation of about 2.5 to 3 Hz is superimposed, which is only inadequately represented in the simulation model. As already observed in Figure 3, this appears to be an air resonance vibration, which is specified for the BO 105 with a frequency of approx. 16 rad/s (= 2.55 Hz)[20].

The expectation of increased inherent static stability in forward flight can be confirmed by this result. The divergence observed in hover flight in Figure 3 and Figure 4 after completion of the control inputs practically no longer occurs in this flight condition (see pitch rate from second 4). In general, other phenomena come into play in forward flight, such as a more or less pronounced Dutch Roll oscillation, which must be taken into account by appropriate modelling.

The coupling responses generally show a higher simulation quality in the roll rate (up to second 6) than was observed in the simulation calculations in the hover condition. Comparing the results of the PWD model with those of the dynamic inflow model, it should be noted that the optimisation results in a slight improvement with regard to the gradients as well as the amplitudes. The simulations of both models show a good agreement with the measurement data after the completion of the control inputs.

In the pitch rate (from second 6), a considerable improvement of the simulation quality can be observed by optimising the PWD model. As described, the wake

This work is licensed under the Creative Commons Attribution International License (CC BY). Copyright © 2021 by author(s).

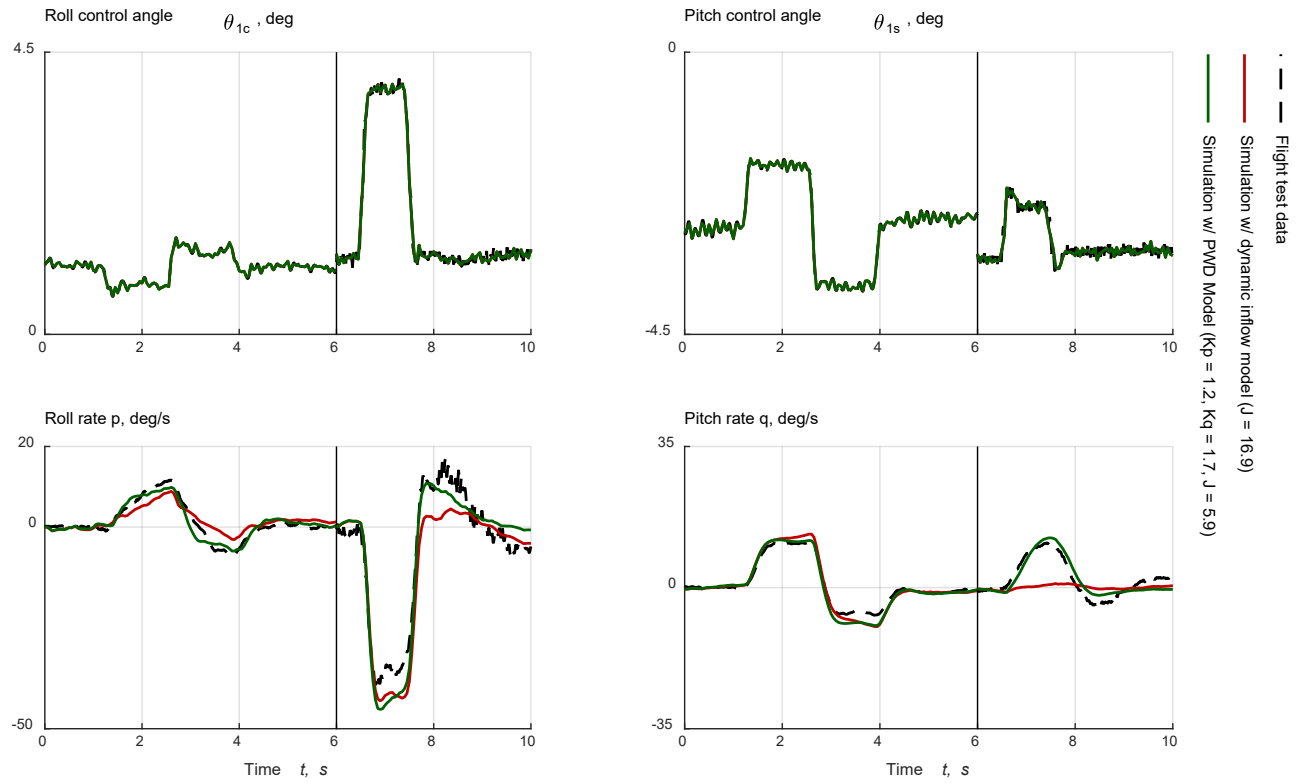

Figure 5 Simulation result with optimised PWD model – BO 105, forward flight 80 kts, swashplate control, doublet/pulse.

distortion theory does not provide an explanation for this degree of effectiveness. Reasons for the sensitivity of the model also in horizontal flight are obviously other effects, which are insufficiently represented in the overall model and correlated with the mode of action of the PWD model. Of course, this improvement of the simulation quality can be accepted and the parameters in the overall model can be implemented accordingly, but it must be stated that this improvement is not due to the actually intended description of the wake distortion effect. In this sense, such a model improvement represents a certain departure from phenomenological analytical modelling.

However, consideration of the optimised parameters shows that the theory can be confirmed by the calculation to the extent that the parameter values have an overall tendency to decrease with increasing horizontal speed. With K_p = 1.2 and K_q = 1.7, especially the parameter K_p, which weights the pitch coupling due to a roll control input, is significantly lower than determined in hover flight. The improvement of the cost function in this flight condition amounts to ΔJ = 65%.

7. DISCUSSION

The Parametric Wake Distortion model was able to meet the objectives for the application of the system identification procedure in a non-linear simulation environment. Especially the possibility of interpreting the results on the basis of theoretical preliminary investigations represents a valuable basis for verification.

The basic findings of the application of the method to the PWD problem are as follows:

- The evaluation of individual physical effects is possible and effective by means of the applied method.
- The prerequisite for this is a high overall model quality, as well as a hierarchical order of the considered sub-model in the overall modelling, which allows the resulting deficits to be assigned to the investigated effect and quantified using the optimisation procedure.
- The optimisation procedure is able to achieve a considerable improvement in the simulation quality under certain boundary conditions without significantly affecting the physically plausible basis of the overall modelling.
- The combination of the method with the model allows several parameters to be processed simultaneously and thus enables results, which only have the required significance in the combination of the parameters, as is the case with the presented problem of the axis coupling modelling.

Thus, the approach of an improvement of the simulation quality with simultaneous evaluation of the involved physical effects of the considered system could be successfully implemented.

The application to the simulation of the BO 105 helicopter underlines the capability of the approach under the mentioned aspects. In hover flight (see Figure 4) the coupling response could be significantly improved, especially the pitch rate as a reaction of a roll control input. Furthermore, the parameters could be determined in a relevant value range with regard to the theoretical

This work is licensed under the Creative Commons Attribution International License (CC BY). Copyright © 2021 by author(s).

prediction. In this case, a convincing subjective increase of the simulation quality about the roll axis could only be achieved to a limited extent. On the one hand, this is due to the already higher simulation quality from the outset (which can be seen in the results of the simulation using the dynamic inflow model), on the other hand due to obviously existing deficits of the global modelling, which cannot be attributed to the Parametric Wake Distortion effect.

The latter, the susceptibility of the optimisation to other physical effects and model inaccuracies is a major concern when coupling parametric optimisation methods to a meaningful physics based nonlinear modelling.

The results in forward flight (Figure 5) underline the applicability of the model approach beyond the limits of the theoretically predicted range of use. However, some caution is necessary here in the application and in the evaluation of the results in order not to be subject to misinterpretations in the evaluation of the physical effects actually involved.

With the application of the presented identification procedure, it could be shown which benefit the implementation of physically plausible parametric models offers within a non-linear simulation environment. However, it also shows the difficulties and the fields of improvement and future work. The inaccuracies of the global helicopter model have an impact on the performance of the procedure. To identify the exact model parts whose inaccuracies couple with the Parametric Wake Distortion optimisation would complete the applicability of the procedure as a whole.

REFERENCES

[1] Peters, David A.: How Dynamic Inflow Survives in the Competitive World of Rotorcraft Aerodynamics. Journal of the American Helicopter Society, 54(1), 2009. https://doi.org/10.4050/JAHS.54.011001

[2] Pitt, Dale M. und David A. Peters: Theoretical Predicion of Dynamic Inflow Derivatives. In: Proceedings of the 6th European Rotorcraft Forum, Bristol, England, 1980.

[3] Peters, David A. und Ninh HaQuang: Dynamic Inflow for Practical Applications. Journal of the American Helicopter Society, 33(4), 1988.

[4] Tischler, Mark B., Peter G. Hamel und Jan A. Mulder (editors): System Identification for Integrated Aircraft Development and Flight Testing. RTO Meeting Proceedings MP-11. NATO Research and Technology Organization, 1999.

[5] Hamel, Peter G. (editor): Rotorcraft System Identification. AGARD Advisory Report AR-280. NATO Advisory Group for Aerospace Research & Development, 1991.

[6] Fu, Kuang-Huang and Martin Marchand: Helicopter System Identification in the Frequency Domain. In: Proceedings of the 9th European Rotorcraft Forum, Stresa, Italy, 1983.

[7] Kaletka, Jürgen, Mark B. Tischler, Wolfgang von Grünhagen and Jay W. Fletcher: Time and Frequency Domain Identification and Verification of BO 105 Dynamic Models. In: Proceedings of the 15th European Rotorcraft Forum, Amsterdam, The Netherlands, 1989.

[8] Fu, Kuang-Huang and Jürgen Kaletka: Frequency-Domain Identification of BO 105 Derivative Models with Rotor Degrees of Freedom. In: Proceedings of the 16th European Rotorcraft Forum, Glasgow, UK, 1990.

[9] Krämer, Philipp: Hybridmodellierung und Systemidentifizierung der nichtlinearen Hubschrauber-Flugdynamik, DLR Forschungsbericht 2006-14, ISSN 1434-8454, Köln, 2006.

[10] Krämer, Philipp, Bernard Gimonet und Wolfgang von Grünhagen: A systematic Approach to nonlinear Rotorcraft Model Identification. Aerospace Science and Technology (AST), 6(8), 2005.

[11] Prouty, Raymond W.: Helicopter Performance, Stability, and Control. Krieger Publishing Company, 2. Edition, 2001. ISBN 978-1575242095

[12] Leishman, J. Gordon: Principles of Helicopter Aerodynamics. Cambridge University Press, Cambridge, 2nd edition, 2006. ISBN 978-1107013353.

[13] Joglekar, M. und Robert G. Loewy: An Actuator-Disk Analysis of Helicopter Wake Geometry and the Corresponding Blade Response. Technical Report 69-66, U.S. Army Aviation Laboratories, 1970.

[14] Keller, Jeffrey D.: An Investigation of Helicopter Dynamic Coupling using an Analytical Model. In: Proceedings of the 21st European Rotorcraft Forum, St. Petersburg, Russia, 1995.

[15] Keller, Jeffrey D. und Howard C. Curtiss, Jr.: Modeling the Induced Velocity of a Maneuvering Helicopter. In: Proceedings of the 52nd AHS Annual Forum, Washington, DC, 1996.

[16] Rosen, Aviv und Aharon Isser: A new Model of Rotor Dynamics during Pitch an Roll of a Hovering Helicopter. In: Proceedings of the 50th AHS Annual Forum, Washington, DC, 1994.

[17] Arnold, Uwe T. P., Jeffrey D. Keller, Howard C. Curtiss, Jr. und Günther Reichert: The Effect of Inflow Models on the Predicted Response of Helicopters. In: Proceedings of the 21st European Rotorcraft Forum, St. Petersburg, Russia, 1995.

[18] Hamers, Mario und Wolfgang von Grünhagen: Nonlinear Helicopter Model Validation Applied to Realtime Simulations. In: Proceedings of the 53rd AHS Annual Forum, Virginia Beach, VA, 1997.

[19] Grünhagen, Wolfgang von: The BO 105 Database. DLR Report, 2002.

[20] Bittner, Walter: Flugmechanik der Hubschrauber. Springer Verlag, Berlin, 4. Auflage, 2014. ISBN 978-3642542855.

This work is licensed under the Creative Commons Attribution International License (CC BY). Copyright © 2021 by author(s).